Polymer 49 (2008) 5363–5372

Contents lists available at ScienceDirect

Polymer

journal homepage: www.elsevier.com/locate/polymer

Feature Article

Review on morphology development of immiscible blends in confined shear flow

P. Van Puyvelde, A. Vananroye, R. Cardinaels, P. Moldenaers*

Katholieke Universiteit Leuven, Department of Chemical Engineering, Leuven Materials Research Centre, W. de Croylaan 46, B-3001 Leuven, Belgium

ARTICLE INFO

Article history:
Received 27 June 2008
Received in revised form 25 August 2008
Accepted 27 August 2008
Available online 11 September 2008

Keywords:
Confinement
Blend morphology
Single droplet behaviour

ABSTRACT

The bulk dynamics of immiscible polymer blends during flow is relatively well understood, especially when the system contains Newtonian components. Recently, a number of studies have focused on flow of immiscible blends in confined geometries. In that case, the morphology development is not only affected by the material characteristics and the type of flow, but also by the degree of confinement. Here, we present an overview on the morphology development in immiscible two-phase blends in confined shear flow. Firstly, we focus on the typical microstructures that are observed in confined dilute blends. Secondly, in order to understand those peculiar morphologies, the systematic studies on single droplets in confined shear flow are reviewed. In addition to the experimental work, theoretical, phenomenological, and numerical models that include the effects of confinement are discussed.

1. Introduction

The past decade has witnessed a rapid development of micro- and nanotechnology that is being used in a broad variety of applications. This has led to a multitude of integrated microdevices that combine, for instance, pumps, separation units, and valves into a lab-on-a-chip [1]. Quite rarely, the fluids of interest in such devices are simple single-phase liquids. On the contrary, many systems in chemical and/or biochemical technology consist of multiphase fluids, often containing components with a complex rheology. From a technological point of view, microchannel flows are often used to generate small volumes of emulsions with well-controlled droplet sizes and droplet size distributions. These droplet-based multiphase flows have been utilized in processes such as, for instance, microencapsulation, micromixing, and microreaction [2]. In the latter case, the small droplets are almost ideal chemical reactors characterized by fast heat transfer and efficient mass transfer. In literature, various other applications have also been described, and undoubtedly, many more will follow [2].

To optimize these microfluidic applications, a scientific understanding of the relationships between the rheology of the components, the kinematic conditions, and the microstructure development in confined geometries is essential. This morphology development is however complex and influenced by a multitude of parameters. In order to fully understand the underlying physics, several model type problems have been studied. Earlier research primarily focused on confined channel flow, a topic that was thoroughly reviewed by Olbricht [3]. In the last decade, studies on *confined shear flow* are prevailing, which will be the topic of this review. Moreover, we will only consider *fully immiscible fluid–fluid mixtures* although it was shown that confinement can have a drastic effect on the phase behaviour of a blend. For instance, Binder and co-workers demonstrated, using Monte-Carlo simulations, that in ultrathin films, thinner than the screening length of excluded volume interactions, a dramatic enhancement of compatibility occurs as compared to the corresponding bulk system (e.g. [4,5]). Moreover, it was demonstrated that the standard concepts of the theory of polymeric systems, such as the Flory–Huggins theory [6], fail in highly confined conditions [5]. The situation becomes even more complicated when differences in wettability between the confining walls and the blend constituents are taken into account (e.g. [7–10]). Most of these studies are performed by means of Monte-Carlo simulations under quiescent conditions, and many of the conclusions are experimentally difficult to assess. Therefore, we will not take wetting effects into account in this review.

In the non-confined case, the structural evolution in immiscible systems is relatively well understood. Especially in the case of dilute blends consisting of Newtonian components and subjected to shear flow, both the morphology development and the rheological behaviour are quite well established. For these dilute systems, the blend morphology consists of a droplet–matrix structure. In the absence of buoyancy and inertia effects, the droplet behaviour is governed by two dimensionless numbers: p and Ca. p represents the viscosity ratio of the blend, being the

* Corresponding author. Tel.: +32 16 32 23 59; fax: +32 16 32 29 91.
E-mail address: paula.moldenaers@cit.kuleuven.be (P. Moldenaers).

0032-3861
doi:10.1016/j.polymer.2008.08.055

viscosity of the droplet phase η_d with respect to that of the matrix phase η_m. Ca is the capillary number defined as the ratio between the deforming hydrodynamic stresses and the restoring interfacial stresses ($Ca = R\eta_m\dot{\gamma}/\sigma$, with R, $\dot{\gamma}$, and σ the droplet radius, shear rate and interfacial tension respectively). The single droplet behaviour in Newtonian–Newtonian systems has been thoroughly reviewed by Rallison [11], Stone [12], and more recently by Guido and Greco [13]. The rheological behaviour of these simple blends and its relation with the microstructure have been extensively investigated both experimentally and theoretically [14]. However, most industrial systems consist of more complex viscoelastic components, and the single droplet behaviour in such blends has therefore received a great deal of attention [13,15]. For these systems, two additional dimensionless numbers are introduced for each component: the Deborah number ($De = \sigma\Psi_1/2R\eta^2$, with Ψ_1 the first normal stress coefficient and η the fluid viscosity), and the ratio N_2/N_1, with N_1 and N_2 the first and second normal stress differences of the fluid [13,16]. It has been shown that matrix viscoelasticity substantially influences the steady and transient droplet dynamics when $De \geq 1$. Droplet viscoelasticity seems to have less effect on the droplet behaviour, at least at non-critical conditions. The role of N_2 on the droplet dynamics is less clear [13,15,17–20]. To obtain a material with improved properties, the final goal is often to generate very small droplets dispersed in the matrix. Therefore, particular interest is going towards compatibilization and morphology stabilization of immiscible blends [15]. At higher concentrations, hydrodynamic interactions and coalescence become important, and fibrillar and cocontinuous structures can be generated [17]. Component viscoelasticity, the presence of compatibilizers, and concentration all add additional complexities to the system, and therefore, the relationships between rheology and morphology for these systems are not yet fully understood under bulk conditions.

In the case of microfluidic flow of blends, at least one dimension d of the flow system is on the micron scale and therefore could become comparable to the characteristic size of the dispersed phase (characterized by the droplet diameter $2R$). This confinement effect could drastically influence the physics of the rheological and morphological changes during flow. In the field of microrheometry, the different instrumental approaches can roughly be divided into two groups [21]. On the one hand, there is interfacial rheometry, which typically involves deformations in domains of a few molecular dimensions. On the other hand, literature focuses on microrheometry, which has recently evolved rapidly due to the possibility to fabricate microscale devices [21]. These microrheological developments are however beyond the scope of this review, and an extensive overview is given by Waigh [22].

This review discusses the effect of confinement on the morphological changes in immiscible blends consisting of Newtonian components in simple shear flow. In the first part, the peculiar morphologies observed in dilute confined blends are discussed. In order to understand the evolution of these morphologies during flow, single droplet dynamics together with an evaluation of the various single droplet models is reviewed in the second part. Concerning the experimental work, literature mainly reports on studies that use in situ time resolved methods, such as light microscopy, to gain insight into the relationship between flow and structure development. These in situ studies have undoubtedly the advantage that the morphology evolution is examined during flow, in contrast to 'postmortem' techniques such as scanning electron microscopy in which the morphology can only be viewed after the sample has been solidified. In situ observation of the morphology of industrial systems is however often difficult. Limited transparency and contrast, as well as a too fine microstructure can hamper the observations. Therefore, model systems with appropriate viscoelastic and optical properties were selected by several research teams such that the resulting microstructure can be studied using light microscopy.

2. Morphology development in dilute confined blends consisting of Newtonian components

The first systematic experimental studies in confined shear flow were conducted on dilute blends, rather than on single droplets. Concentration however adds a complication to the structural dynamics since deformation and breakup will compete with coalescence. So far, only systems containing Newtonian components were studied in confined shear flow. The early experiments by Migler [23] revealed a richness of morphological phenomena. Migler reported a transition from a dispersed droplet state to a string-like state in confined flow. Under identical kinematic conditions in bulk flow, this system would display a droplet–matrix structure with only slightly deformed ellipsoidal droplets. The transition occurs when the size of the dispersed droplets becomes comparable to the gap width. A typical example is shown in Fig. 1. It displays the morphology evolution which is microscopically investigated in a Linkam shearing cell after a decrease in shear rate. Initially, coalescence causes an increase in the average droplet size (A and B). After some time, a self-organization into pearl necklace structures occurs (B and C). This pearl necklace pattern, which was observed by Migler for the first time in liquid–liquid systems, is seen as a transient stage between the droplet state and the string state. Next, the aligned droplets coalesce into strings (D) and even ribbons (E and F), as indicated by the arrow in Fig. 1(E). All strings have the same width W in the vorticity direction. The string stabilization is caused by a suppression of the Rayleigh instability [24] due to confinement. Although the nearby presence of the walls is essential to keep the strings intact, it is not sufficient. Flow provides an additional stabilization, as is also the case in the unconfined situation [25]. In fact, it was experimentally shown that when the flow is stopped, most of the strings eventually breakup into droplets [23]. Hence, both confinement and flow are necessary to prevent string breakup. The suppression of Rayleigh instabilities by the presence of the walls was confirmed both experimentally and numerically. Son et al. [26] experimentally investigated the stability of a polymeric thread embedded in a quiescent matrix confined between two parallel walls. For a ratio of thread diameter to gap spacing between 0.33 and 0.77, an initially axisymmetric thread becomes nonaxisymmetric, the growth rate of the instabilities decreases, and the wavelength increases as compared to the unconfined situation. Extremely confined strings remained stable over the entire experimental timescale. Hagedorn et al. [27] used a Lattice-Boltzmann model to simulate the breakup of threads in a tube and between parallel plates. The authors reported that confinement has a similar effect in both type of geometries. They also pointed out the importance of fluid–substrate thermodynamic interactions (wetting) in the stabilization of these confined threads.

Pathak et al. [28] stated that the transition of bulk-like behaviour to string formation in a confined flow is not only affected by changing the shear rate for a fixed gap spacing. They demonstrated that the morphology development is additionally influenced by the volume fraction of the blend. These authors presented a morphology diagram for $p = 1$ that describes the microstructure in confined polydimethylsiloxane/polyisobutylene emulsions in the parameter space of composition and shear rate for a gap spacing d of 36 μm. Besides the formation of strings and pearl necklaces which are seen by Pathak et al. [28] as stable morphologies, they reported the organization of droplets in distinct layers. The physics behind the formation of the layered microstructure is not completely understood at present. However, the number of layers decreases with increasing degree of droplet confinement and it was suggested that this is related to two migration effects [28]: drift of

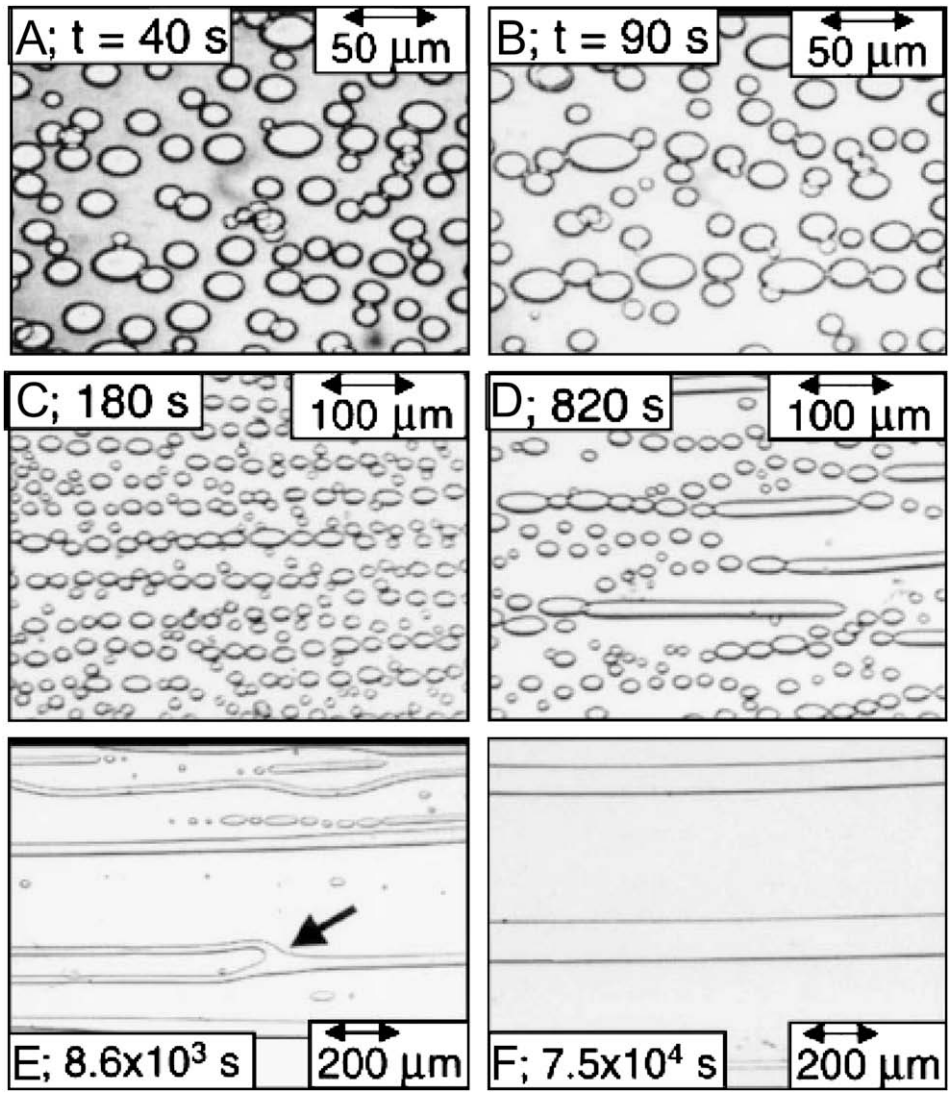

Fig. 1. Kinetics of the droplet to string transition in a polydimethylsiloxane/polyisobutylene blend with a mass ratio of 0.28 dispersed phase and viscosity ratio of unity. Images are taken in the velocity–vorticity plane (←: flow; ↑: vorticity) at a gap spacing d of 30 µm. The shear rate is reduced at $t = 0$ s from the droplet regime ($\dot{\gamma} = 4\ s^{-1}$) to the string regime ($\dot{\gamma} = 2.5\ s^{-1}$). (A) and (B) Increase in droplet size. (B) and (C) Pearl necklace formation in the velocity direction. (D) Coalescence into strings. (E) and (F) String–string coalescence into ribbons. Reprinted figure with permission from Migler KB. Physical Review Letters 86, p. 1023 (2001) [23]. Copyright (2001) by the American Physical Society.

droplets from the walls towards the centre (wall migration) and migration towards the walls due to shear-induced droplet collisions, which occurs in a direction perpendicular to the streamlines. Only a few articles describe experimental studies on wall migration of droplets in emulsions [29–31]. For instance, King and Leighton [29] performed experiments on dilute emulsions with a low viscosity ratio in a Couette flow. They reported drift of droplets from the walls and accumulation of droplets near the centre of the gap. A steady-state droplet distribution was reached when a shear-induced gradient diffusivity balances the wall migration. Good agreement between their experimental results and a combination of a linearized form of the migration velocity for a single droplet [32] and a shear-induced dispersion model [33] was seen [29]. Hudson [31] extended the analysis of King and Leighton [29] by removing the restriction of linearizing the migration velocity. He performed migration experiments in a parallel plate device and stated that the wall migration effect is significant, even when the droplets are 100 times smaller than the gap. Collision processes in liquid–liquid dispersions have been reviewed by Chesters [34]. An expression for the collision frequency per unit volume was given by Smoluchowski [35], assuming that the droplets are monodisperse spheres which follow the basic streamlines in simple shear flow. Pathak et al. [28] argued that geometrical confinement accentuates the wall migration effect and reduces the number of collisions per timescale. For a confined droplet in shear flow, they deduced expressions for the timescales relevant to droplet collisions, based on the original Smoluchowski equation [35], and to droplet migration based on the theory of Chan and Leal [32]. It was reported [28] that the ratio T of the collision timescale to the migration timescale increases with decreasing shear rate. For shear rates where $T < 1$, a two-layer microstructure was seen. In this case, collisions occur more frequently than migration causing droplets to accumulate in two distinct layers. When $T \sim O(1)$, the timescales for collision and migration are similar. Under these conditions, a single layer was reported [28].

The deformation of droplets in the parameter space of confinement, shear rate and concentration was also investigated. For example, Pathak and Migler [36] reported on the effect of confinement on droplet deformation in a blend with 9.7 wt% dispersed phase and a viscosity ratio of unity. The authors stated that Taylor's single droplet theory [37,38] still provides a reasonable estimate of the deformation for $Ca < 0.1$, as long as the droplet

diameter is smaller than the gap size (confinement ratio $2R/d < 1$). For droplet dimensions exceeding the gap size, squashed droplets are formed below the critical capillary number for bulk breakup, and stable strings with a constant width above the bulk critical capillary number. Similar experiments were performed by Vananroye et al. [39] on blends with 1–10 wt% dispersed phase and by Tufano et al. [40] in blends with 10–30 wt% dispersed phase. Both research teams showed that for larger capillary numbers, the deformation of droplets is already affected by the presence of the walls when the confinement ratio $2R/d$ is approximately 0.3. They additionally reported that for the confinement ratios under investigation (up to $2R/d = 0.55$), the mean droplet size is still governed by the relations that describe non-confined situations. Vananroye et al. [39] demonstrated that not only the width of the strings in the vorticity direction, but also the width of droplets on pearl necklaces is constant during shear flow irrespective of the droplet size. A typical example is given in Fig. 2 in which the droplet width W in the vorticity direction is shown as a function of the droplet diameter $2R$ for droplets in a 5 wt% emulsion sheared at 0.38 s^{-1}. As can be seen in Fig. 2 for a gap spacing d of 40 μm, the width W of droplets remains constant above a critical confinement ratio $2R/d$ of roughly 0.4. Tufano et al. [40] showed that this constant width phenomenon already occurs before the formation of ordered pearl necklace structures, and that the critical degree of confinement at which such wall effects become important increases with decreasing shear rate.

When flow is arrested, the relaxation of droplets on pearl necklaces could be affected by the presence of the walls. This was investigated by Vananroye et al. [39] for droplets in a 5 wt% blend after a shear rate of 0.38 s^{-1}. Their results indicate that confinement does not have an effect on droplet relaxation, at least for the conditions under investigation, where the largest droplet had a confinement ratio $2R/d$ of 0.55.

3. Single droplet dynamics in confined shear flow

During flow, droplets undergo morphological changes such as deformation, retraction, breakup, and coalescence. In order to understand the peculiar structures discussed in the previous section, relationships between the flow and the structure dynamics in a confined environment are needed at the level of single droplets. To the authors' knowledge, the effect of confinement on shear-induced coalescence on a two-drop level is unexplored. However, droplet deformation, orientation, retraction, and breakup have been investigated experimentally, theoretically, and numerically in confined shear flow.

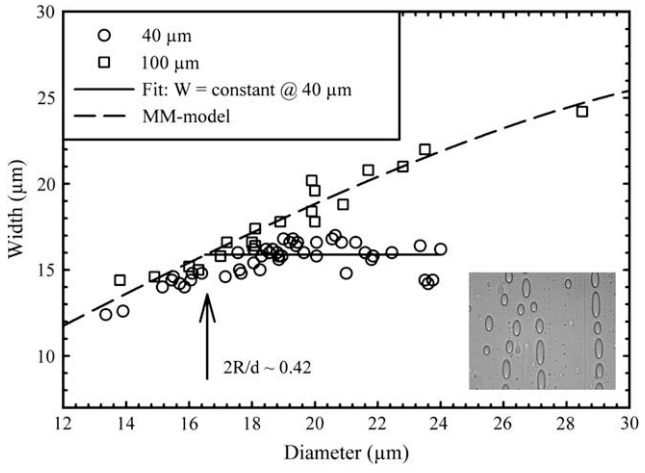

Fig. 2. Droplet width W as a function of the undeformed droplet diameter $2R$ at a shear rate of 0.4 s^{-1} and a viscosity ratio of 0.47 (5 wt% polyisobutylene in polydimethylsiloxane) for gap spacings d of 40 μm and 100 μm. Experiments were performed using a Linkam parallel plate shearing cell. The dashed line represents the prediction of the Maffettone and Minale model for single ellipsoidal droplets in bulk shear flow [41,42]. Reprinted figure with permission from Vananroye et al. [43]. Copyright (2006) by Applied Rheology.

3.1. Theoretical background

From a theoretical point of view, various attempts have been made to extend existing models to include the effect of confinement on the dynamics of single droplets in shear flow. The shape of moderately deformed droplets is generally described by the three droplet axes L, B and W, assuming an ellipsoid. The droplet orientation is expressed by means of the orientation angle θ, which is the angle between the longest droplet axis L and the flow direction. The magnitude of the deformation is commonly quantified by means of the deformation parameter $D = L - B/L + B$. A schematic representation of a deformed droplet in a simple shear flow is shown in Fig. 3.

For nearly spherical droplets, a theoretical solution for the shape of a droplet interacting with two parallel shearing walls was obtained by Shapira and Haber [44]. They solved the momentum and continuity equation with the Lorentz reflection approximation [45], using only three reflections. Therefore, the results are only applicable for small confinement ratios $2R/d$. An analytical expression for the droplet deformation D_{SH}, of the first order in Ca, was obtained:

$$D_{SH} = D_{Taylor}\left[1 + C_s\frac{1+2.5p}{1+p}\left(\frac{R}{d}\right)^3\right] \quad (1)$$

with

$$D_{Taylor} = \mathrm{Ca}\frac{16+19p}{8(1+p)}\sin\theta\cos\theta \quad (2)$$

C_s is a parameter that depends on the relative position of the droplet between the walls and grows considerably when the droplet approaches one of the two walls. In all experimental studies, care was taken to position the droplet symmetrically between the two confining walls. For that case, a value of C_s of 5.699 was reported [44]. D_{Taylor} is the deformation parameter obtained from the Taylor small-deformation bulk theory [37,38]. Eq. (1) predicts that the additional effect of the walls on the magnitude of the deformation scales with the ratio of droplet radius R to gap width d to the power 3. The droplet shape however, remains ellipsoidal and unaltered with respect to the Taylor small-deformation prediction

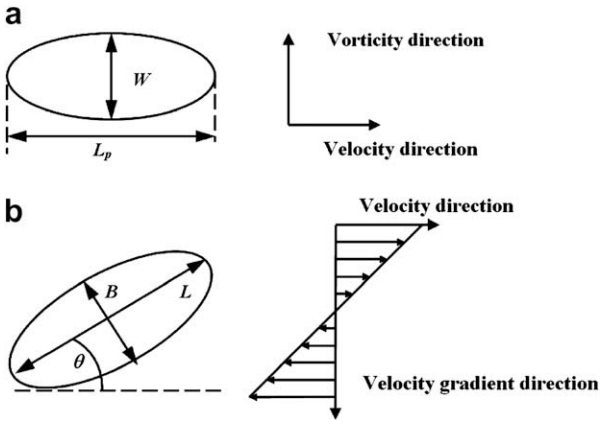

Fig. 3. Schematic representation of a deformed droplet with the geometrical parameters in shear flow: (a) velocity–vorticity plane (top view); (b) velocity–velocity gradient plane (side view).

for bulk shear flow. As in this first-order bulk theory, a constant orientation angle θ of 45° is predicted. Chan and Leal [32] studied wall effects on the deformation of a sheared droplet when both the droplet and the matrix fluid are second-order fluids. They did not obtain explicit expressions for the droplet deformation as a function of viscosity and confinement ratios. But for the Newtonian limit, the values for the shape factor C_s, calculated at $R/d = 0.1$ for three different droplet locations within the gap, are in agreement with the values of Shapira and Haber [44].

The Taylor bulk theory is derived for small deformations and viscosity ratios around 1. To extend the applicability of Eq. (1) to viscosity ratios different from 1 and to large deformations, Vananroye et al. [46] proposed to replace the Taylor bulk deformation parameter D_{Taylor} with the steady-state deformation expression D_{MM} of the model of Maffettone and Minale [41,42]. This leads to a combined MMSH model with deformation parameter D_{MMSH}:

$$D_{\text{MMSH}} = D_{\text{MM}}\left[1 + C_s\frac{1+2.5p}{1+p}\left(\frac{R}{d}\right)^3\right] \tag{3}$$

with

$$D_{\text{MM}} = \frac{f_{2\text{MM}}\text{Ca}}{\sqrt{f_{1\text{MM}}^2 + \text{Ca}^2} + \sqrt{f_{1\text{MM}}^2 + \left(1 - f_{2\text{MM}}^2\right)\text{Ca}^2}} \tag{4}$$

$$f_{1\text{MM}} = \frac{40(p+1)}{(2p+3)(19p+16)} \tag{5}$$

$$f_{2\text{MM}} = \frac{5}{2p+3} + \frac{3\text{Ca}^2}{2+6\text{Ca}^2} \tag{6}$$

The original Maffettone–Minale model [41,42] is a phenomenological model for the dynamics of a single Newtonian drop in a Newtonian matrix subjected to a generic bulk flow. It has been proven that this model satisfactorily describes the droplet dynamics in bulk shear flow [41,46–48]. The droplet shape is assumed to remain ellipsoidal at all times and is described by a second rank symmetric, positive definite tensor **S**. The dynamics of **S** is determined by the competing actions of viscous flow and interfacial tension. The parameters $f_{1\text{MM}}$ and $f_{2\text{MM}}$ are derived so that the model recovers the small-deformation limit of Taylor [37,38]. Similar to the approach of Vananroye et al. [46], the Shapira–Haber theory was extended to describe the deformation of confined droplets in systems with one viscoelastic component [49]. In bulk shear flow, droplet and especially matrix viscoelasticity can substantially alter the droplet deformation and orientation [13]. Therefore, the bulk Taylor deformation parameter was replaced with the deformation parameter obtained from bulk phenomenological deformation models for systems containing one viscoelastic component, such as the modified Minale model [18,19]. With this approach, only the effect of component viscoelasticity on the unbounded deformation is taken into account, while the Shapira–Haber correction factor for wall effects is derived for Newtonian components.

Despite of its relative success in describing the droplet deformation, a major drawback of the Shapira–Haber theory [44] and its aforementioned extensions is the fact that no predictions of the droplet dynamics under transient flow conditions can be made. Recently, the phenomenological Maffettone–Minale model [41,42] was extended by Minale to the case of a generic confined flow [50]. The dynamic equation for **S** of the Maffettone–Minale model was kept unaltered but adapted expressions for the functions f_1 and f_2, which now also depend on the ratio R/d, were proposed. Thereto, the confined version of the model is forced to recover the small-deformation limits of Shapira and Haber [44]. In that way, the ratio between f_1 and f_2 was imposed. Minale [50] proposed expressions for f_1 and f_2, consisting of the Maffettone–Minale parameters $f_{1\text{MM}}$ and $f_{2\text{MM}}$ corrected with a confinement factor that is proportional to $(R/d)^3$:

$$f_1 = \frac{f_{1\text{MM}}}{\left(1 + C_s\left(\frac{R}{d}\right)^3 f_{1c}\right)} \tag{7}$$

$$f_2 = f_{2\text{MM}}\left(1 + C_s\left(\frac{R}{d}\right)^3 f_{2c}\right) \tag{8}$$

To resolve the remaining degree of freedom in the expressions for f_1 and f_2, the steady-state model predictions were fitted to the experimental results of Vananroye et al. [46] and Sibillo et al. [51]. Expressions for the correction factors f_{1c} and f_{2c} as a function of viscosity ratio p were obtained for p between 0.3 and 5. With this confined version [50] of the Maffettone–Minale model [41,42], the droplet deformation as well as the droplet orientation can be obtained. In addition, the droplet response to transient flow conditions, such as e.g. start-up or cessation of shear flow, can be predicted. Critical conditions for breakup can also be derived from the model, in which an indefinite droplet deformation is associated with supercritical conditions.

Although providing predictions on the droplet deformation and orientation under a broad range of conditions, the quantitative applicability of the available models for confined droplet dynamics remains restricted to ellipsoidal droplet shapes, and hence, to low values of Ca and low confinement ratios. In order to cover the entire spectrum of capillary numbers, including conditions close to breakup, numerical simulations are needed. In addition, velocity and pressure fields, which become accessible with numerical simulations, could provide valuable information to unravel the underlying physics of the observed peculiar phenomena (see further). Janssen and Anderson [52] used a Boundary-Integral-Method (BIM) to simulate the 3D droplet deformation and breakup of a Newtonian droplet in a Newtonian matrix for confined shear flow at a viscosity ratio of 1. To take into account the presence of the walls, they used an additional wall term in the Green's functions, as derived by Jones et al. [53] for a droplet in a Poiseuille flow between two parallel plates. Simultaneously, Renardy [54] used a Volume-Of-Fluid method (VOF) to simulate the 3D dynamics of a Newtonian droplet in a Newtonian matrix at a confinement ratio $2R/d$ of 0.68 and a viscosity ratio of 1. In these simulations, the VOF method was combined with the parabolic reconstruction of the interface shape in the surface tension force (PROST [55]) or alternatively the continuous surface formulation (CSF [56]) with the piecewise linear interface reconstruction scheme (PLIC [57]). Recently, Janssen and Anderson extended their Boundary-Integral-Method for droplets between two parallel walls to the non-unit viscosity ratio case [58].

3.2. Comparison with experimental evidence

3.2.1. Steady-state droplet deformation and orientation

From an experimental point of view, a large number of studies on droplet deformation in confined shear flow have been performed. They show a wide variety of wall effects on the single droplet dynamics. The first evaluation of the Shapira–Haber theory [44] was performed by Sibillo et al. [51], for a system consisting of equiviscous Newtonian components. A high precision sliding plate device, equipped with a microscope that translates together with the moving plate, was used to visualize a single droplet in a bounded shear flow. As demonstrated in Fig. 4, good agreement between the theoretical deformation parameter (Eq. (1)) and experimental results was obtained. Even for confinement ratios $2R/d$ as high as

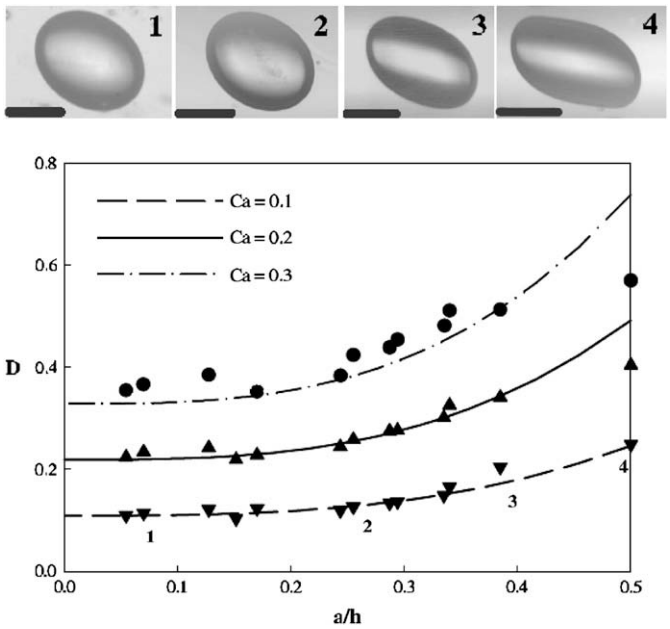

Fig. 4. Comparison between the experimental deformation parameter and Eq. (1) as a function of the ratio of droplet radius to gap width $a/h(=R/d)$ at $p=1$. Microscopic images in the velocity–velocity gradient plane at Ca = 0.1 for a/h determined by the corresponding numbers in the graph. Reprinted figure with permission from Sibillo V, Pasquariello G, Simeone M, Cristini V, and Guido S. Physical Review Letters 97, 054502 (2006) [51]. Copyright (2006) by the American Physical Society.

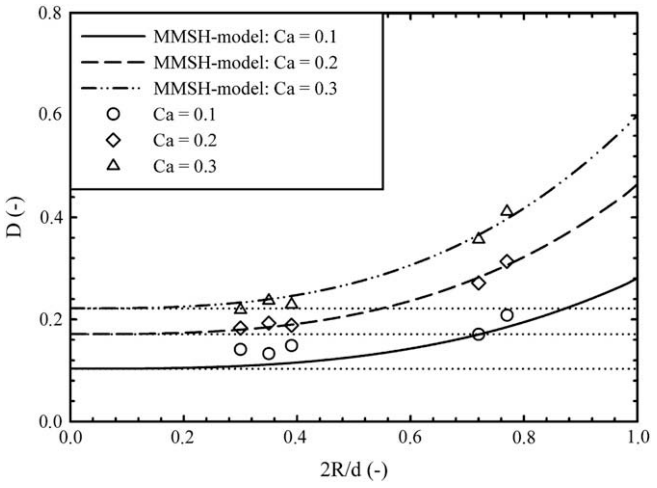

Fig. 5. Comparison between the experimental deformation parameter and Eq. (3) (MMSH model) as a function of the confinement ratio $2R/d$ at $p=5.2$. Reprinted figure with permission from Vananroye et al. [46]. Copyright© 2007 by The Society of Rheology, Inc. All rights reserved.

0.8, where the mathematical solution method used to obtain Eq. (1) is no longer valid, experiments and predictions nicely match. Whereas the Shapira–Haber theory [44] only predicts confinement effects on the magnitude of the deformation, at high confinement ratios, Sibillo et al. [51] clearly observed distortions from the ellipsoidal droplet shape, as shown by the microscopy images in Fig. 4. Vananroye et al. [46] performed a systematic study on the steady-state droplet deformation in confined shear flow, using a counter-rotating parallel plate device. They studied systems with viscosity ratios between 0.3 and 5. It was shown that, above a confinement ratio $2R/d$ of 0.3, both the droplet deformation and the droplet orientation towards the flow direction are systematically increased with respect to the bulk case. It was demonstrated that the differences between the bulk and the confined droplet deformation augment with increasing viscosity ratio. This trend is correctly captured by the Shapira–Haber model [44] and Eq. (3) was shown to do a relatively good job in describing the experimental deformation parameter, especially at the highest viscosity ratios. An example of a comparison between Eq. (3) and the experimental results is shown in Fig. 5.

By extending the Maffettone–Minale model to include confinement effects, Minale [50] was able to quantitatively predict the droplet axes L, B, and W and the droplet orientation angle θ for confined droplets in Newtonian–Newtonian systems, as long as the deviation from an ellipsoidal shape remained limited [50]. As an example, Fig. 6 shows a comparison between the experimentally obtained dimensionless droplet axes and the model predictions for a viscosity ratio of 2. Both experiments [46,59] and the model [50,59] show that wall effects on the orientation angle are more pronounced at the lowest viscosity ratios, whereas the deformation is more affected at high viscosity ratios.

The steady-state deformation in confined droplet–matrix systems with one viscoelastic component was studied by Verhulst et al. [49]. At a viscosity ratio of 1.5 and a Deborah number of 1, they observed similar trends for the confinement effect as in fully Newtonian systems. To describe the deformation parameter as a function of confinement ratio, the bulk Taylor deformation parameter in Eq. (1) was replaced with that of the bulk phenomenological modified Minale model [18,19] for systems with one viscoelastic component. Although only the effects of component viscoelasticity on the unbounded droplet deformation were taken into account, the model predictions nicely matched the experimental results.

A quantitative comparison between the steady state experimentally observed deformation at different Ca-numbers and the simulations of Janssen and Anderson [52] has been performed by Vananroye et al. [60], for a viscosity ratio of 1. Contrary to the confined Minale model [50] and the Shapira–Haber model [44], the BIM is capable of predicting the full sigmoidal steady-state droplet shape, as illustrated in Fig. 7. The simulations also predict an increase in droplet deformation and more orientation towards the flow direction with increasing degree of confinement, which is all in line with experimental observations. It is proposed by the authors that the changed droplet dynamics under confined

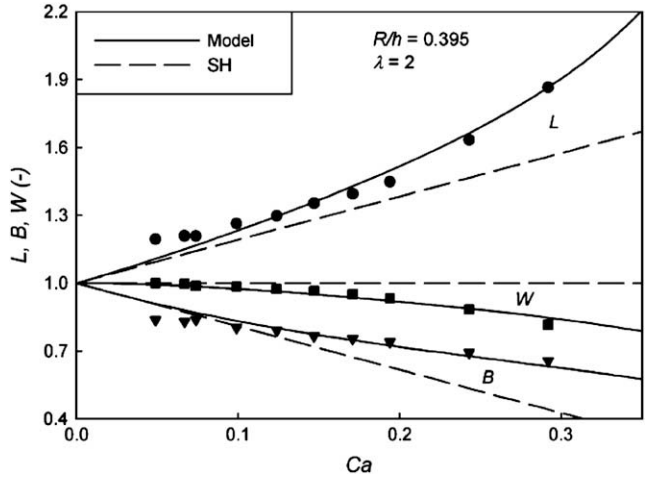

Fig. 6. Comparison between the experimental dimensionless droplet axes (dots), the Shapira–Haber theory (dashed lines) and the confined Minale model (full lines) at $p=2$ and $2R/d=0.79$. With kind permission from Springer Science + Business Media: Rheologica Acta, A phenomenological model for wall effects on the deformation of an ellipsoidal drop in viscous flow, 47, 2008, p. 667, Minale M., Figure 6 [50]. Copyright (2008).

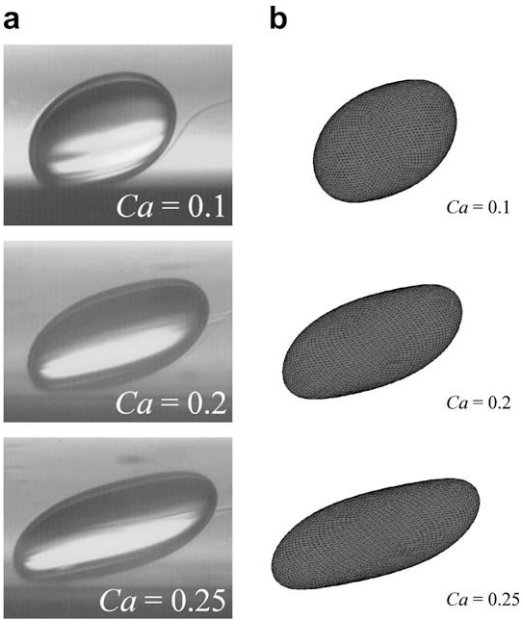

Fig. 7. Comparison between experimental data (a) and BIM simulation results (b) for the steady-state droplet shape in the velocity–velocity gradient plane at $p = 1$ and $2R/d = 0.83$. Reprinted with permission from Vananroye et al. [60]. Copyright (2008) by The American Institute of Physics.

conditions is mainly caused by the changed pressure profile outside the droplet. A comparison between numerical simulations and experimental data at non-unit viscosity ratios is not yet available in literature. The VOF method was recently extended to take into account the viscoelasticity of the components [61]. Therefore, 3D simulations of confined droplet dynamics during shear flow in systems containing viscoelastic components have become accessible, but so far comparison with experimental data is restricted to bulk conditions [20].

3.2.2. Droplet dynamics during start-up of shear flow

In addition to the increased steady-state droplet deformation and droplet orientation in confined shear flow, substantial changes in the droplet dynamics during transient flow conditions were also observed. For the simple case of Newtonian–Newtonian systems, this time-dependent deformation and orientation were experimentally investigated by Sibillo et al. [51] for a viscosity ratio of 1 and by Vananroye et al. [47] for a broad range of viscosity ratios. At low values of the capillary number, the droplet deformation and orientation evolve monotonously towards their steady-state values [47]. Longer shearing times are required however, to reach steady state [47]. Vananroye et al. demonstrated that the Minale extension for confinement [50] of the Maffettone–Minale model [41,42] at least qualitatively captures these trends. A comparison between model predictions and experimental data for three different viscosity ratios is shown in Fig. 8. For highly confined droplets sheared under near-critical conditions, one or more overshoots in the droplet deformation have been experimentally observed [51]. In addition, the timescales required to reach steady-state conditions increase with an order of magnitude compared to the bulk case. These overshoots become less pronounced when the viscosity ratio is high [47]. The Minale extension for confinement [50] of the Maffettone–Minale model [41,42] is not capable of reproducing the experimentally observed overshoots [47].

On the other hand, with both the VOF and BIM simulation methods discussed in Section 3.1, quantitative agreement with the oscillation transients was obtained for a viscosity ratio of 1 [54,60]. A comparison between the experimental results and VOF simulations is shown in Fig. 9. The maximum in the deformation can be explained by the fact that the tips of the stretching droplet are pushed away from the walls. Then, the droplet orientation angle reduces, and the droplet experiences a much weaker flow and retracts [52,54]. Contrary to the situation in bulk shear flow, a high shear rate exists in the space between drop tip and wall, with substantial recirculation flows on both sides of the droplet [52,54]. Since it was shown that the droplet orientation is more sensitive to wall effects at low viscosity ratios [59], more pronounced overshoots are expected for these systems, in agreement with the experimental results [47].

3.2.3. Droplet retraction upon cessation of shear flow

Whereas the droplet deformation is affected by the presence of the walls for confinement ratios $2R/d$ of 0.3 and higher, one might expect, based on the dilute blends studies [39], that the retraction of single droplets upon cessation of flow is less sensitive to confinement. Vananroye et al. [47] investigated this for viscosity ratios between 0.3 and 2 and observed that only highly confined droplets relax slower compared to unconfined droplets. This is in agreement with the observations of Son and

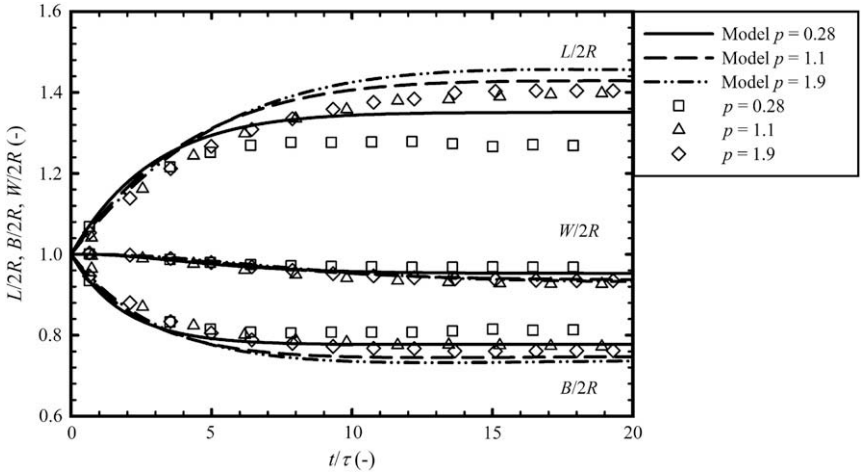

Fig. 8. Effect of viscosity ratio on start-up transients at low Ca. Comparison between experimental data (symbols) and predictions of the confined Minale model (lines) for the dimensionless droplet axes at $2R/d = 0.73$ and $\mathrm{Ca} = 0.2$. The absolute time t is scaled with the characteristic emulsion time τ. Reprinted figure with permission from Vananroye et al. [47]. Copyright© 2008 by The Society of Rheolgy, Inc. All rights reserved.

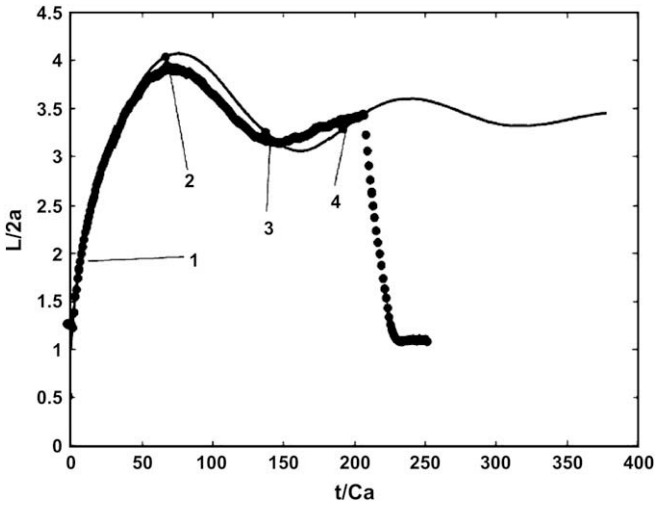

Fig. 9. Dynamics of droplets during start-up of flow at high Ca. Comparison between experimental data and numerical simulations with the VOF method at $p = 1$, Ca = 0.4 and $2R/d = 0.68$. a = R. With kind permission from Springer Science + Business Media: Rheologica Acta, The effects of confinement and inertia on the production of droplets, 46, 2007, p. 521, Renardy Y., Figure 2 [54]. Copyright (2007).

Migler [62] who studied the retraction of axisymmetrical droplets, which were obtained from a retracting imbedded fibre, confined between two parallel plates. For their system, consisting of two polymer melts at a viscosity ratio of 0.25, wall effects on the relaxation only start to appear at a confinement ratio $2R/d$ of 0.5. Vananroye et al. [47] compared the droplet relaxation to the predictions of the confined Minale model [50], as illustrated in Fig. 10 for a viscosity ratio of 1. According to the model, the effect of confinement on droplet relaxation is already substantial at lower degrees of confinement, which is not in line with the experiments. At high degrees of confinement however, the Minale model predictions are in good agreement with the data. At very high confinement ratios, not only the relaxation kinetics, but also the qualitative relaxation behaviour is altered by the presence of the walls. Son and Migler [62] mentioned the transition from an axisymmetrical droplet towards an ellipse flattened in the direction perpendicular to the walls. Cardinaels et al. [63] noticed that the sigmoidal droplet shapes at high confinement ratios result in a deviation from the well-known exponential relaxation curves. These authors also studied droplet relaxation in systems with one viscoelastic component. Under bulk conditions, matrix viscoelasticity retards the droplet relaxation, while hardly any influence of droplet viscoelasticity on the relaxation kinetics was noticed. Similar to fully Newtonian systems, confinement causes the droplets to retract slower. For blends containing a viscoelastic matrix however, the relaxation kinetics is less influenced by confinement. This is most probably due to the slower droplet relaxation in a viscoelastic matrix, which provides more time for the matrix fluid to be squeezed out between the plates and the droplet.

3.2.4. Droplet breakup

When the capillary number is sufficiently increased, droplets might breakup. For a viscosity ratio of 1, Sibillo et al. [51] demonstrated that confinement hardly affects the critical capillary number that describes breakup in bulk flow conditions. A systematic study of the effect of confinement on the near-critical breakup process for a broad range of viscosity ratios was conducted by Vananroye et al. [64]. For a viscosity ratio of 1, the observations of Sibillo et al. [51] were confirmed. However, for viscosity ratios below 1, Vananroye et al. showed that the critical capillary number increases with increasing confinement, indicating that confined droplets are stabilized by the presence of the walls. At viscosity ratios above 1, it was seen that the critical capillary number decreases, thus confinement promotes breakup. These authors also showed that even droplets with viscosity ratios above 4, which are unbreakable in bulk shear flow, can still be broken in confined conditions. The experimental results are summarized in Fig. 11 together with the predictions of the confined Minale model [50]. Although the model can qualitatively predict the observed trends, it is not quantitative. This is not surprising since at breakup conditions, the droplet shape is far from an ellipsoidal one.

For confinement ratios $2R/d$ very close to 1, Sibillo et al. [51] showed an interesting new breakup mode in which three droplets with comparable droplet sizes are formed, in contrast with bulk breakup where the central fragments are generally much smaller than the main daughter drops. The experimentally observed transition from binary to ternary breakup [51,59] was reproduced by both the BIM [52] and the VOF simulations [54]. Renardy [54]

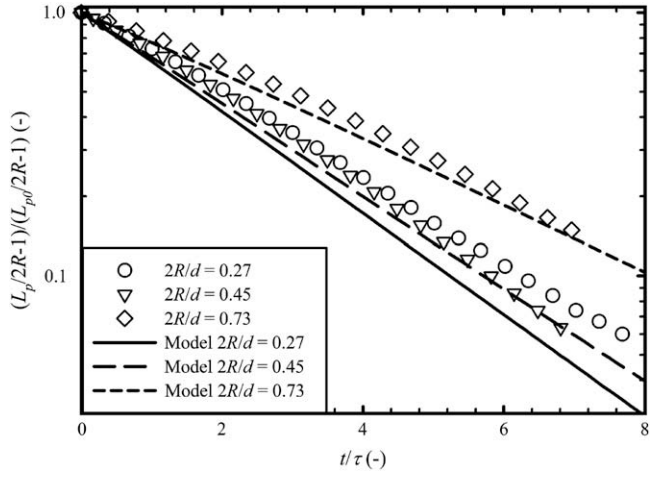

Fig. 10. Effect of confinement ratio on droplet retraction. Comparison between experimental data and predictions of the confined Minale model during relaxation after steady shear flow at Ca = 0.3 with $p = 1$. L_p and L_{p0} represent the major axis of the ellipsoid's projection on the velocity–vorticity plane on time t and 0 respectively. Reprinted figure with permission from Vananroye et al. [47]. Copyright© 2008 by The Society of Rheolgy, Inc. All rights reserved.

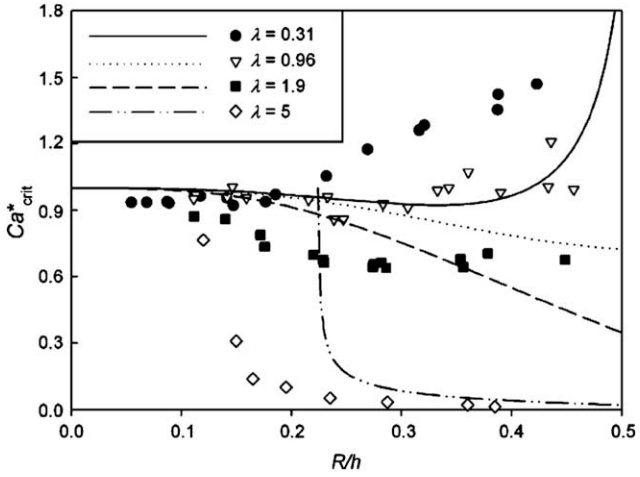

Fig. 11. Effect of viscosity ratio and confinement on the droplet breakup criterium. Comparison between experimental data (symbols) and predictions of the confined Minale model (lines). The critical Ca number is scaled with its bulk value. With kind permission from Springer Science + Business Media: Rheologica Acta, A phenomenological model for wall effects on the deformation of an ellipsoidal drop in viscous flow, 47, 2008, p. 667, Minale M., Figure 13 [50]. Copyright (2008).

attributes this to the increased shear rate at the drop tips, which prevents them from evolving into dumbbells, as in unbounded shear flow. Recently, Cardinaels et al. [59] have demonstrated that the number of equally sized daughter drops increases with confinement ratio. In addition, the transition from bulk breakup to confined breakup with multiple neckings was shown to shift towards more confined conditions for systems with a high viscosity ratio or containing a viscoelastic matrix.

4. Conclusions

In this review, the morphology development of immiscible blends confined between two shearing parallel plates is discussed. An overview is given on the different peculiar structures that are observed in dilute confined blends containing Newtonian components. Depending on the gap spacing, volume fraction, and shear rate, a richness of morphological states such as layered structures, pearl necklaces, strings, ribbons, and squashed droplets appear. In order to gain more insight into the formation of such structures, relationships between the flow and the structure dynamics in a confined environment are needed at the level of single droplets. Confinement can substantially alter the droplet deformation, droplet orientation and droplet breakup during steady-state and transient shear flow. Under rather mild conditions of shear and confinement, the analytical theories and models for confined droplets are capable of describing the droplet shape and droplet orientation rather accurately. Recently, 3D numerical simulations of the droplet behaviour in confined shear flow have emerged. It has already been demonstrated for a viscosity ratio of 1 that such simulations accurately predict the droplet dynamics and the sigmoidal droplet shape under a wide range of conditions. Moreover, the simulated pressure and velocity fields provide valuable insights into the underlying physics. For more concentrated systems however, a complete understanding of the morphology development in a confined geometry is not yet obtained. Additionally, real industrial blends typically consist of viscoelastic components, are often compatibilized, and are processed in rather complex flow fields. Although preliminary results on the behaviour of confined single droplets in systems with viscoelastic components are available, the effect of confinement on the behaviour of these more complex systems or under complex flow conditions is largely unexplored.

Acknowledgements

FWO Vlaanderen (Ph.D. fellowship for R. Cardinaels and Postdoctoral Fellowship for A. Vananroye) and onderzoeksfonds K.U. Leuven (GOA 03/06 and GOA 09/002) are gratefully acknowledged for financial support.

References

[1] Stone HA, Stroock AD, Ajdari A. Annual Review of Fluid Mechanics 2004;36:381–411.
[2] Shui L, Eijkel JCT, van den Berg A. Advances in Colloid and Interface Science 2007;133(1):35–49.
[3] Olbricht WL. Annual Review of Fluid Mechanics 1996;28:187–213.
[4] Binder K. Advances in Polymer Science 1999;138:1–89.
[5] Cavallo A, Muller M, Binder K. Journal of Physical Chemistry B 2005; 109(14):6544–52.
[6] Flory PJ. Principles of polymer chemistry. Ithaca, N.Y.: Cornell University Press; 1953.
[7] Binder K, Muller M, Albano EV. Physical Chemistry Chemical Physics 2001;3(7):1160–8.
[8] Evans R. Journal of Physics: Condensed Matter 1990;2(46):8989–9007.
[9] Swift MR, Owczarek AL, Indekeu JO. Europhysics Letters 1991;14(5):475–81.
[10] Dreyfus R, Tabeling P, Willaime H. Physical Review Letters 2003;90(14): 1445051–4.
[11] Rallison JM. Annual Review of Fluid Mechanics 1984;16:45–66.
[12] Stone HA. Annual Review of Fluid Mechanics 1994;26:65–102.
[13] Guido S, Greco F. Rheology Reviews 2004:99–142.
[14] Tucker CL, Moldenaers P. Annual Review of Fluid Mechanics 2002;34:177–210.
[15] Van Puyvelde P, Moldenaers P. Rheology Reviews 2005:101–45.
[16] Greco F. Journal of Non-Newtonian Fluid Mechanics 2002;107(1–3):111–31.
[17] Van Puyvelde P, Moldenaers P. Rheology-morphology relationships in immiscible polymer blends. In: Harrats C, Thomas S, Groeninckx G, editors. Micro- and nanostructured multiphase polymer blend systems: phase morphology and interfaces. USA: CRC Press, Taylor & Francis; 2006.
[18] Minale M. Journal of Non-Newtonian Fluid Mechanics 2004;123(2–3):151–60.
[19] Verhulst K, Moldenaers P, Minale M. Journal of Rheology 2007;51(2):261–73.
[20] Verhulst K, Cardinaels R, Moldenaers P, Renardy Y, Afkhami S. Journal of Non-Newtonian Fluid Mechanics 2008; doi:10.1016/j.jnnfm.2008.06.007.
[21] Clasen C, McKinley GH. Journal of Non-Newtonian Fluid Mechanics 2004; 124(1–3):1–10.
[22] Waigh TA. Reports on Progress in Physics 2005;68:685–742.
[23] Migler KB. Physical Review Letters 2001;86(6):1023–6.
[24] Tomotika S. Proceedings of the Royal Society of London Series A 1935;150:322–37.
[25] Khakhar DV, Ottino JM. International Journal of Multiphase Flow 1987;13(1): 71–86.
[26] Son Y, Martys NS, Hagedorn JG, Migler KB. Macromolecules 2003;36(15): 5825–33.
[27] Hagedorn JG, Martys NS, Douglas JF. Physical Review E 2004;69(5):056312.
[28] Pathak JA, Davis MC, Hudson SD, Migler KB. Journal of Colloid and Interface Science 2002;255(2):391–402.
[29] King MR, Leighton DT. Physics of Fluids 2001;13(2):397–406.
[30] Hollingsworth KG, Johns ML. Journal of Colloid and Interface Science 2006;296(2):700–9.
[31] Hudson SD. Physics of Fluids 2003;15(5):1106–13.
[32] Chan PCH, Leal LG. Journal of Fluid Mechanics 1979;92(May):131–70.
[33] Loewenberg M, Hinch EJ. Journal of Fluid Mechanics 1997;338:299–315.
[34] Chesters AK. Chemical Engineering Research and Design 1991;69(4): 259–70.
[35] Smoluchowski MZ. Journal of Physical Chemistry 1917;92:129–68.
[36] Pathak JA, Migler KB. Langmuir 2003;19(21):8667–74.
[37] Taylor GI. Proceedings of the Royal Society of London Series A 1932;138:41–8.
[38] Taylor GI. Proceedings of the Royal Society of London Series A 1934;146: 501–23.
[39] Vananroye A, Van Puyvelde P, Moldenaers P. Langmuir 2006;22:2273–80.
[40] Tufano C, Peters GWM, Meijer HEH. Langmuir 2008;24(9):4494–505.
[41] Maffettone PL, Minale M. Journal of Non-Newtonian Fluid Mechanics 1998;78(2–3):227–41.
[42] Maffettone PL, Minale M. Journal of Non-Newtonian Fluid Mechanics 1999;84(1):105–6.
[43] Vananroye A, Van Puyvelde P, Moldenaers P. Applied Rheology 2006;16: 242–7.
[44] Shapira M, Haber S. International Journal of Multiphase Flow 1990;16(2): 305–21.
[45] Happel J, Brenner H. Low Reynolds number hydrodynamics. Leiden: Noordhoff International Publishing; 1973.
[46] Vananroye A, Van Puyvelde P, Moldenaers P. Journal of Rheology 2007;51(1): 139–53.
[47] Vananroye A, Cardinaels R, Van Puyvelde P, Moldenaers P. Journal of Rheology 2008;52(6).
[48] Guido S, Minale M, Maffettone PL. Journal of Rheology 2000;44(6):1385–99.
[49] Verhulst K, Cardinaels R, Moldenaers P. Steady state droplet deformation and orientation during shear flow in blends with one viscoelastic component: bulk and confined conditions. In: Polymer Processing Society Europe/Africa regional meeting, Göteborg; 2007.
[50] Minale M. Rheologica Acta 2008;47:667–75.
[51] Sibillo V, Pasquariello G, Simeone M, Cristini V, Guido S. Physical Review Letters 2006;97(5):054502.
[52] Janssen PJA, Anderson PD. Physics of Fluids 2007;19(4):043602.
[53] Jones RB. Journal of Chemical Physics 2004;121(1):483–500.
[54] Renardy Y. Rheologica Acta 2007;46(4):521–9.
[55] Renardy Y, Renardy M. Journal of Computational Physics 2002;183(2):400–21.
[56] Brackbill JU, Kothe DB, Zemach C. Journal of Computational Physics 1992; 100(2):335–54.
[57] Li J, Renardy YY, Renardy M. Physics of Fluids 2000;12(2):269–82.
[58] Janssen PJA, Anderson PD. Journal of Computational Physics 2008; 227(20):8807–19.
[59] Cardinaels R, Vananroye A, Verhulst K, Moldenaers P. Separate and combined influence of confinement and component viscoelasticity on single droplet behavior during shear flow. Polymer Processing Society 24th Annual Meeting, Salerno; 2008.
[60] Vananroye A, Janssen PJA, Anderson PD, Van Puyvelde P, Moldenaers P. Physics of Fluids 2008;20(1):013101.
[61] Khismatullin D, Renardy Y, Renardy M. Journal of Non-Newtonian Fluid Mechanics 2006;140(1–3):120–31.
[62] Son Y, Migler KB. Polymer 2002;43(10):3001–6.
[63] Cardinaels R, Verhulst K, Moldenaers P. Drop shape dynamics during shear flow in blends with one viscoelastic component: bulk and confined conditions. Ninth European symposium on polymer blends, Palermo; 2007.
[64] Vananroye A, Van Puyvelde P, Moldenaers P. Langmuir 2006;22:3972–4.

Peter Van Puyvelde is Associate Professor in the group of Applied Rheology and Polymer Processing of the Department of Chemical Engineering of the K.U. Leuven. He obtained his Ph.D. from the same institute, working on the use of rheo-optical methods in the study of morphology development in immiscible polymer blends. In 2002, he was post-doc in the Materials Technology Group headed by Prof. H.E.H. Meijer. His current research focuses on flow-induced microstructures in polymeric systems in general and on flow-induced crystallization in particular.

Ruth Cardinaels studied at the Katholieke Universiteit Leuven from 2000 to 2005, where she received a master's degree in Chemical Engineering. She is now doing a Ph.D. on the morphology and rheology of concentrated polymer blends with one viscoelastic component under supervision of Prof. Paula Moldenaers in the group of Applied Rheology and Polymer Processing of the Department of Chemical Engineering of the Katholieke Universiteit Leuven.

Anja Vananroye studied at the Katholieke Universiteit Leuven from 1998 to 2003, where she received a master's degree in Chemical Engineering. She obtained her Ph.D. from the same institute, working on the structure development in polymer blends during flow in confinements. She is now a post-doctoral researcher in the group of Applied Rheology and Polymer Processing of the Katholieke Universiteit Leuven, where she continues her work on compatibilized blends in confined flow.

Paula Moldenaers is Full Professor at the Department of Chemical Engineering of the Katholieke Universiteit in Leuven and is Head of the Laboratory of Applied Rheology and Polymer Processing. Her research focusses on the rheology and morphology of complex fluids. Paula Moldenaers received the Annual Award of the British Society of Rheology in 1991 and the Publication Award of the Society of Rheology in 1997 (with I. Vinckier and J. Mewis). She is a member of the Royal Flemish Academy of Belgium for Arts and Sciences.